Journal of Membrane Science 487 (2015) 135–140

Contents lists available at ScienceDirect

Journal of Membrane Science

journal homepage: www.elsevier.com/locate/memsci

Cryogenic air separation at low pressure using MFI membranes

Pengcheng Ye*, Danil Korelskiy, Mattias Grahn, Jonas Hedlund

Chemical Technology, Luleå University of Technology, SE-971 87 Luleå, Sweden

ARTICLE INFO

Article history:
Received 27 January 2015
Accepted 15 March 2015
Available online 4 April 2015

Keywords:
Zeolite membrane
Cryogenic temperature
Air separation
Low pressure

ABSTRACT

Ultra-thin MFI membranes were for the first time evaluated for air separation at low feed pressures ranging from 100 to 1000 mbar at cryogenic temperature. The membrane separation performance at optimum temperature at all investigated feed pressures was well above the Robeson upper bound for polymeric membranes at near room temperature. The O_2/N_2 separation factor at optimum temperature increased as the feed pressure was decreased and reached 5.0 at 100 mbar feed pressure and a membrane temperature of 67 K. The corresponding membrane selectivity was 6.3, and the O_2 permeance was as high as 8.6×10^{-7} mol m^{-2} s^{-1} Pa^{-1}. This permeance was about 100 times higher than that reported for promising polymeric membranes. The membrane selectivity and high O_2 permeance was most likely a result of O_2/N_2 adsorption selectivity. The increase in O_2/N_2 separation factor with decreasing pressure and temperature was probably due to increased adsorption selectivity at reduced temperature. This work has demonstrated the potential of MFI zeolite membranes for O_2/N_2 separations at cryogenic temperature.

1. Introduction

Development of more efficient methods for separation of various gas mixtures are currently of tremendous interest. Membrane gas separation technology is one such method that is already applied in industrial scale for H_2 recovery, CO_2 separation, dehydration of air and natural gas, and air separation [1]. For the latter application, polymeric membranes have been developed for separation of O_2 from air. Most of these membranes show high selectivity but low permeability, i.e., low flux [2]. Robeson has investigated the performance of different polymeric membranes and found a trade-off between the desired selectivity and permeability. The best polymeric membranes with high selectivity had relatively low permeability, and vice versa. This trade-off is known as the Robeson selectivity–permeability upper bound [3] and it was updated in 2008 [4]. It is here worth pointing out that for industrial applications, materials with as high permeability as possible, possessing sufficient selectivity, are of major interest [2]. In other words, a very selective membrane with very low permeability is not very industrially useful. Recently, Carta et al. [5] have reported microporous polymeric membranes with rather high oxygen permeability of 900–1100 Barrer and good O_2/N_2 selectivities of 4.5–6.1.

Zeolite membranes being inorganic porous membranes are known to have high permeabilities in gas separations. Due to the well-defined pore structure, zeolite membranes can also offer high selectivities. In addition, these membranes have high chemical, mechanical and thermal stability, i.e., can potentially be used at both very high and very low temperatures offering a great advantage over polymeric membranes. High temperature applications of zeolite membranes have been studied extensively. On the contrary, scientific reports on gas separation using zeolite membranes at low temperatures are rather scarce. Hong et al. [6] studied CO_2/H_2 separation using SAPO-34 membranes in the temperature range of 253–308 K. At 253 K, the reported CO_2/H_2 separation factor was as high as 110, however the CO_2 flux was only 3 kg m^{-2} h^{-1} even though the trans-membrane pressure difference was as high as 12 bar. Piera et al. [7] separated CO/air at an extremely low CO concentration of 160 ppbv using an MFI-type membrane in the temperature range of 243–303 K. The separation factor was 3.1 with an extremely low CO flux of 1.3×10^{-7} kg m^{-2} h^{-1} at 245 K. Van den Bergh et al. [8] investigated permeation and separation properties of various gases (CO_2, CH_4, N_2, and O_2) and their mixtures, using DDR membranes in the temperature range of 220–373 K. The mixture selectivities increased as temperature was decreased, especially for CO_2/CH_4, CO_2/air and N_2O/air mixtures. The CO_2/CH_4 separation factor was higher than 1000 at temperatures below 250 K. At the same time, the O_2/N_2 selectivity was low amounting to only ca. 2 and the flux was reported as "very low", i.e. lower than 7.8×10^{-2} kg m^{-2} h^{-1} in all cases. Our research group has developed ultra-thin (≈ 0.5 μm) MFI membranes on open graded alumina supports [9]. Due to the low thickness and well-defined pore structure, the membranes can display both high flux and high selectivity. These

* Corresponding author. Tel.: +46 920493161.
E-mail address: pengcheng.ye@ltu.se (P. Ye).

http://dx.doi.org/10.1016/j.memsci.2015.03.063

membranes display excellent performance for CO_2 separation from synthesis gas at high pressure and low temperature [10]. The separation factor for CO_2/H_2 was as high as 32 with a CO_2 flux of 332 kg m^{-2} h^{-1} at 275 K. We have also shown [11] that separation factors exceeding 100 can be reached below 243 K. The greater separation performance of the membranes at lower temperature was attributed to stronger adsorption of CO_2 in the zeolite pores, effectively blocking the transport of H_2. Recently, we have evaluated these membranes for air separation at cryogenic temperatures, i.e., below 123 K and the report [12] is the first on zeolite membrane separation at cryogenic temperature. The experiments were carried out in the temperature range of 77–110 K and the feed pressure was varied between 1–5 bar. Liquid nitrogen was used for cooling, which limited the lowest achievable experimental temperature to 77 K, and no vacuum system was used, which limited the lowest feed and permeate pressures to 1 bar. Helium was used as a sweep gas on the permeate side at a pressure of 1 bar. The membranes were oxygen selective, and when the feed pressure was decreased, the maximum O_2/N_2 separation factor increased whereas the optimum separation temperatures decreased. At the lowest investigated feed pressure of 1 bar and the optimum temperature of 79 K, the highest observed O_2/N_2 separation factor was 3.9, with an O_2 permeance of 6.7×10^{-7} mol m^{-2} s^{-1} Pa^{-1}. We have now installed a vacuum system to enable experiments at reduced pressure, and a cryostat, which enables experiments at temperatures down to 22 K. In the present work, the membranes are evaluated for air separation at significantly lower feed pressures and membrane temperatures than in the previous work [12] using the new experimental set-up. A model for the adsorption in the zeolite pores was also developed to better understand the separation performance of the membranes.

2. Experimental

2.1. Membrane preparation

MFI membranes were prepared on graded porous α-alumina discs (Fraunhofer IKTS, Germany), using a previously reported method [9]. The support had a diameter of 25 mm and was comprised of a 30 μm thick top layer with a pore size of 100 nm and a 3 mm thick base layer with a pore size of 3 μm. The alumina disc was masked and then seeded with a monolayer of MFI crystals of 50 nm in size as described previously [13]. After that, a hydrothermal treatment was carried out, where the seeded support was immersed in a synthesis solution with a molar composition of $3TPAOH:25SiO_2:1450H_2O:100C_2H_5OH$ and kept in the solution at 361 K for 72 h. Thereafter, the membrane was rinsed in a 0.1 NH_3 solution overnight and calcined at 773 K for 6 h at a heating rate of 0.2 K min^{-1} and a cooling rate of 0.3 K min^{-1}.

2.2. Membrane characterization

Adsorption-branch *n*-hexane/helium permporometry [14] was used to characterize the amount of flow-through defects in the membranes. This technique has recently been demonstrated to be an effective and reliable way to evaluate micropore defects down to 0.7 nm [15,16] and mesopore defects [14] in MFI membranes. The procedure for the permporometry characterization is described in our previous work [15].

The morphology of the membranes was characterized by SEM using an FEI Magellan 400 field emission XHR-SEM without any coating of the samples.

2.3. Gas separation measurements

The membrane was mounted in a stainless steel cell and sealed with graphite gaskets (Eriks, the Netherlands). A type T thermocouple inserted inside the cell was used to monitor the temperature. Prior to the gas separation, the membrane was dried in a helium flow at 573 K for 6 h at a heating rate of 1 K min^{-1}.

The separation experiments were carried out using the experimental set-up illustrated in Fig. 1. A flow of 500 ml min^{-1} (purity > 99.999%, AGA) of synthetic air, consisting of 79.2% N_2 and 20.8% O_2, was fed to the membrane at feed pressures of 100 mbar, 400 mbar, 660 mbar and 1000 mbar (at a feed pressure of 100 mbar, the feed flow rate was reduced to 100 ml min^{-1} due to the limited capacity of the vacuum pump). A pressure of 10 mbar, 40 mbar, 66 mbar, or 100 mbar, was applied on the permeate side of the membrane, in order to keep the ratio of feed pressure to permeate pressure at 10. Since the pressure ratio may affect the separation performance, the pressure ratio was kept constant in all experiments. The gas flow rate was controlled by mass flow controllers (Bronkhorst, F-201CV). Vacuum pumps (Pfeiffer Vacuum, MVP 020 and MVP 040) installed after the pressure regulators in the retentate and permeate lines reduced the pressures on both sides of the membrane. The pressures were controlled by dosing valves (Pfeiffer Vacuum, EVN 116). The membrane cell was kept in a custom-built cryostat (ICEoxford UK, DRYICE25K) and the separation temperature could be set at any value ranging from 22 K to 573 K with a deviation of less than 0.05 K. The permeate flow was measured with a mass flow meter (Bronkhorst, F-201CV). The permeate composition was analyzed by a mass spectrometer (GAM 400, InProcess Instruments) every 5 s. A pressure transmitter (Pfeiffer Vacuum, CMR 362) was used to measure the permeate pressure. A column packed with 5A zeolite pellets was dried before the experiment and was used (at room temperature) to adsorb any traces of moisture in the feed gas.

The permeance Π_i (mol m^{-2} s^{-1} Pa^{-1}) was defined as

$$\Pi_i = F_i/(A_{film}\Delta P_i), \quad (1)$$

where F_i is the molar flow rate of component i through the membrane, A_{film} is the membrane area, and ΔP_i is the partial pressure difference of component i.

The separation factor was determined as follows:

$$\beta_{i/j} = (y_i/y_j)/(x_i/x_j), \quad (2)$$

where y_i and x_i are the molar fractions of species i in the permeate and feed streams, respectively.

The membrane selectivity (also referred to as the permeance-based selectivity) was calculated as

$$\alpha_{i/j} = \Pi_i/\Pi_j, \quad (3)$$

where Π_i and Π_j are the permeances of species i and j, respectively.

O_2 and N_2 single gas permeation experiments were also carried out. A stream of 500 ml min^{-1} of O_2 (> 99.999%, AGA) or N_2 (> 99.999%, AGA) was fed to the membrane at 1000 mbar while the permeate side was kept at 100 mbar.

3. Modelling

In order to gain some insight into the experimental observations, the adsorption of N_2 and O_2 was modelled. Heats of adsorption and Langmuir adsorption parameters for N_2 and O_2 in high silica MFI [17] are given in Table 1. It may be expected that the membrane would be N_2 adsorption selective because of the larger heat of adsorption and Langmuir adsorption parameters than those for O_2. However, for mixture adsorption where the

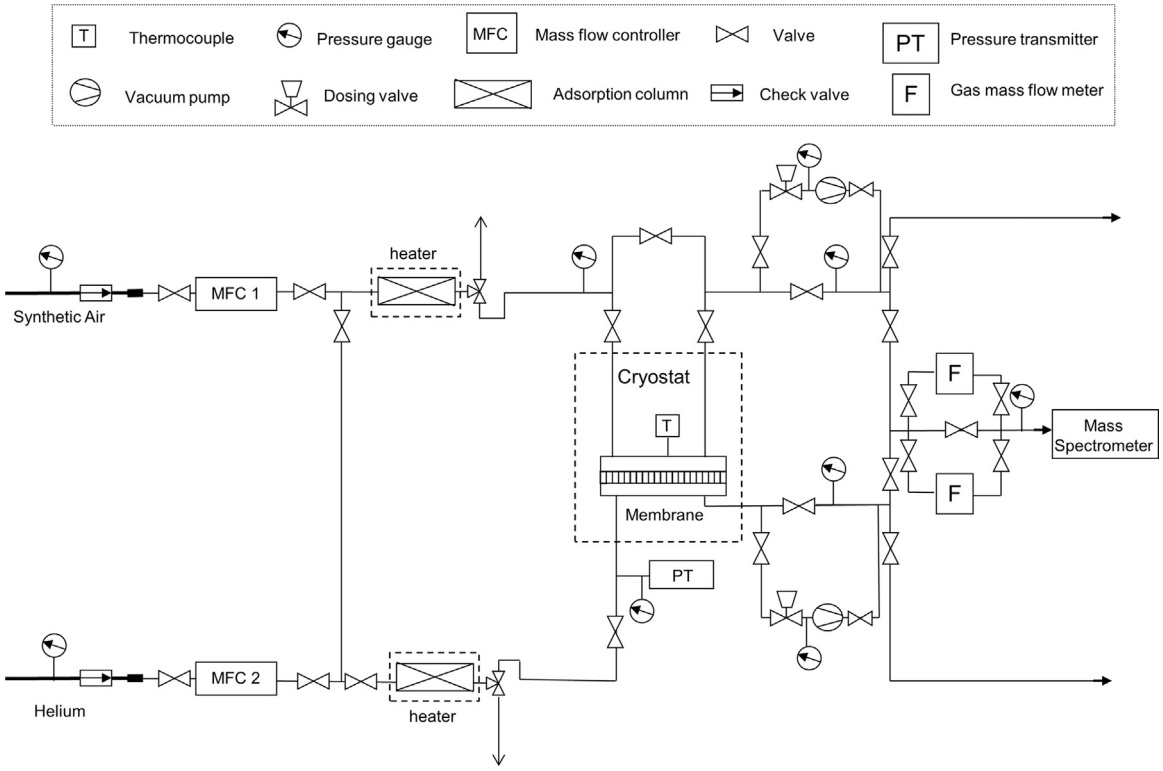

Fig. 1. Gas permeation and separation set-up.

Table 1
Heat of adsorption and Langmuir adsorption parameters for N_2 and O_2 [17].

	ΔH_{ads} (kJ/mol)	b (bar^{-1}) at 303 K
N_2	−17.0	0.277
O_2	−16.3	0.147

Table 2
Helium permeance at equilibrium and relative areas of defects for the membrane, estimated from permporometry data.

p/p_0	Helium permeance at equilibrium (10^{-7} mol m^{-2} s^{-1} Pa^{-1})	Defect width (nm)	Defect interval (nm)	Relative area of defects [a] (%)
0.00	43.15	–	–	–
2.72×10^{-4}	2.86	0.71	–	–
4.55×10^{-4}	2.07	0.73	0.71–0.73	0.07
1.39×10^{-3}	0.95	0.80	0.73–0.80	0.08
1.13×10^{-2}	0.34	1.04	0.80–1.04	0.04
1.39×10^{-1}	0.19	1.78	1.04–1.78	0.005
4.31×10^{-1}	0.14	5.14	1.78–5.14	0.001
			> 5.14	0.0008
			Total	0.20

[a] Area of defects divided by the membrane area.

main difference between the molecules is the size, the isotherms will cross at a certain pressure. It is energetically favorable to adsorb smaller molecules at high loadings since smaller molecules pack more efficiently in the pore system at high loadings [18]. Therefore, at pressures significantly higher than the pressure where the isotherms cross, a reversal in adsorption selectivity may be observed, i.e. an adsorption azeotrope. To illustrate this, adsorption isotherms for O_2 and N_2 at 67 K and 90 K were simulated using the multisite Langmuir model [19]. This model is capable of capturing adsorption azeotropes [18]. The pure component adsorption isotherm is given by [20]

$$p = \frac{\theta}{nb(1-\theta)^n}, \tag{4}$$

where p is the pressure of the adsorbate in gas phase, θ is the fractional coverage (adsorbed loading divided by the saturation loading), b is the Langmuir adsorption parameter, n is the number of adsorption sites one adsorbate molecule occupies. The saturation capacity for N_2 was taken from [21] and that of O_2 was taken as 1.16 times that of N_2 because the volume of an O_2 molecule is ca. 1.16 times smaller than that of a N_2 molecule, as judged from the kinetic diameters of the molecules [3]. b-Values and heat of adsorption reported by Sethia et al. [17] were extrapolated to the temperatures of interest in this work. n was taken as 3 for O_2 and $3 \times 1.16 = 3.48$ for N_2 because a N_2 molecule is ca. 1.16 times larger than a O_2 molecule. The multicomponent version of the multisite Langmuir model is given by [20]

$$\theta_i = n_i b_i p y_i \left(1 - \sum_{j=1}^{N} \theta_j\right)^{n_i}, \tag{5}$$

where index i refers to species i in the mixture and y_i is the gas mole fraction of species i.

4. Results and discussion

Table 2 shows permporometry data for the membrane used in this work. The initial helium permeance at $p/p_0 = 0$, i.e., the helium permeance measured in the absence of n-hexane, was about 43×10^{-7} mol m^{-2} s^{-1} Pa^{-1}. This permeance is about half of that for our best membranes comprised of a film with a total thickness of about 500 nm [9] and the lower permeance indicates that the

total thickness of the film in the membrane used in the present work exceeds 500 nm. However, the defect distribution for this membrane is consistent with that previously reported for high quality membranes prepared by our group [15]. The total amount of defects was only 0.20% of the total membrane surface area indicating a high quality of the membrane. The majority of defects, i.e., 97% of the total amount, were micropore defects smaller than 1 nm in size. As discussed previously [16], these defects are most likely narrow open grain boundaries. In addition, nearly no defects larger than 5 nm in size could be detected.

Fig. 2 shows top view (a) and cross-sectional (b) SEM micrographs of an as-synthesized membrane prepared in the same batch as the membrane used for the separation experiments. The micrographs illustrate that the total film thickness, including support invasion, varies in the range 0.5–1 μm, i.e. the average film thickness exceeds 500 nm, in line with permporometry results. Furthermore, the film is comprised of well-intergrown crystals and no defects can be observed, which also is in-line with permporometry observations.

Fig. 3 shows the simulated single component adsorption isotherms at 67 K and 90 K and it is clear that N_2 shows larger affinity than O_2 for the zeolite at low loadings at both temperatures. However, the isotherms of N_2 and O_2 cross at pressures of ca. 8×10^{-9} and 9×10^{-6} bar at 67 and 90 K, respectively. The partial pressures in the experiments were orders of magnitude higher, and consequently a reversal of the adsorption selectivity, i.e. an adsorption azeotrope, favoring the adsorption of O_2 may be expected in the membrane separation experiments. The multicomponent version of the multisite Langmuir model was used to estimate the adsorption selectivity on the feed side of the membrane, for the same composition as the feed and a total pressure of 100 mbar. The adsorbed loadings were calculated from Eq. (5), and thereafter the O_2/N_2 adsorption selectivities were determined to be 4.2 and 1.8 at 67 and 90 K, respectively. Note that the adoption selectivity increased when the temperature was decreased under the same feed pressure.

Fig. 4 shows the separation results using different feed pressures over the temperature range of 62–106 K. The membrane is oxygen selective as expected from the estimated O_2/N_2 adsorption selectivity. At each feed pressure, a maximum separation factor was observed at an optimum temperature and the separation factor was approaching one at the highest and lowest temperatures studied at all feed pressures. As shown in Table 3, synthetic air condensed at 82 K and 66 K at 1000 and 100 mbar feed pressure, respectively. Condensation of the feed mixture was probably the reason for the drastic drop of separation factor at the lowest investigated temperatures. In order to elucidate these observations, single gas permeation experiments with pure O_2 and N_2 were performed, see Fig. 5. The permeance of N_2 was *higher* than that of O_2 over the entire temperature range despite the fact that the adsorption should favor O_2. This suggests that diffusivity of N_2 should be greater than that of O_2 at all temperatures studied and that the membrane selectivity should mostly emanate from adsorption selectivity. In addition, at the lowest

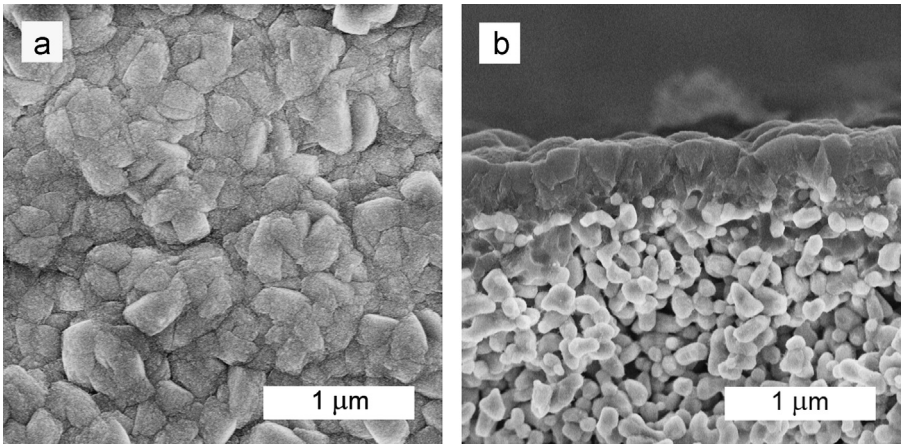

Fig. 2. Top view (a) and cross-sectional (b) SEM images of an as-synthesized MFI membrane.

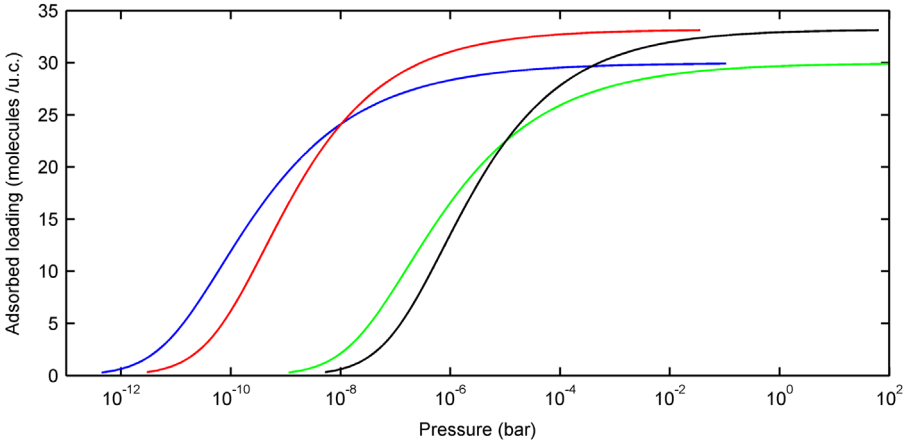

Fig. 3. Simulated single component adsorption isotherms of O_2 (red: 67 K, black: 90 K) and N_2 (blue: 67 K, green: 90 K). (For interpretation of the references to color in this figure legend, the reader is referred to the web version of this article.)

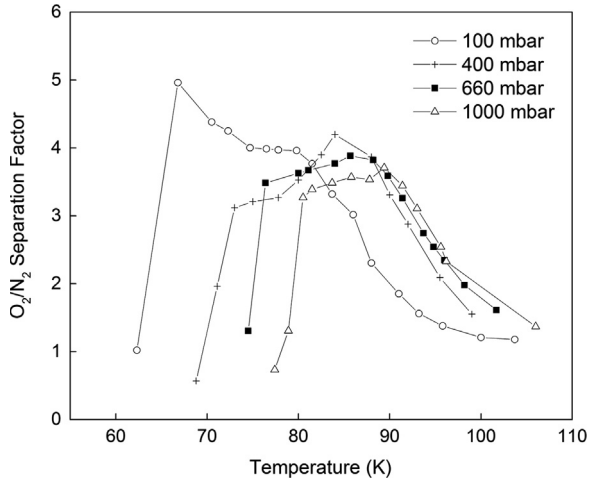

Fig. 4. O_2/N_2 separation factor as a function of temperature for different feed pressures.

Table 3
Dew points of N_2, O_2 and synthetic air at the different feed pressures.

Feed pressure (mbar)	Single gas N_2 dew point (K)	Single gas O_2 dew point (K)	Mixture gas dew point (K)
1000	77.4	90.2	–
1000	–	–	81.6
660	–	–	78.1
400	–	–	74.4
100	–	–	65.9

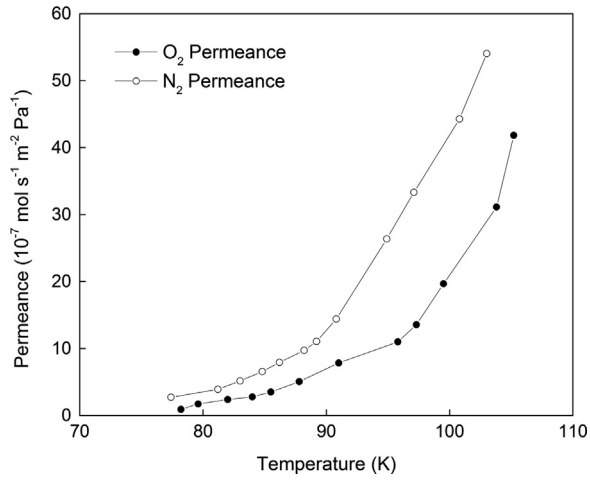

Fig. 5. Single gas permeances for pure O_2 and N_2 as a function of temperature for a feed pressure of 1000 mbar and a permeate pressure of 100 mbar.

temperatures, the single component permeances of both O_2 and N_2 were very low (i.e., below 8.0×10^{-7} mol m^{-2} s^{-1} Pa^{-1}). This is probably a result of condensation of the entire feed at these low temperatures. As shown in Table 3, O_2 condense at 90 K and N_2 at 77 K at 1 bar feed pressure in single component experiments.

At the lowest feed pressure of 100 mbar, a maximum O_2/N_2 separation factor of 5.0 (corresponding to a selectivity of 6.3) with an O_2 permeance of 8.6×10^{-7} mol m^{-2} s^{-1} Pa^{-1} (corresponding to 1025 Barrer) was observed at the optimum

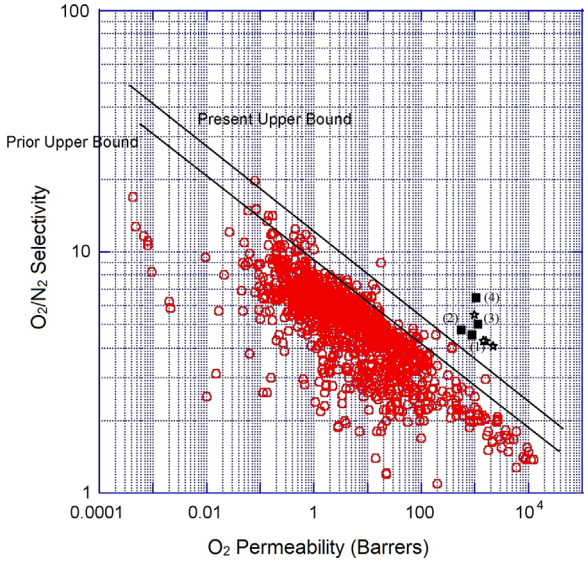

Fig. 6. O_2/N_2 selectivity versus O_2 permeability observed in present work (solid black square) compared to Robeson's 1991 upper bound and 2008 upper bound: (1) 1000 mbar, (2) 660 mbar, (3) 400 mbar, and (4) 100 mbar for feed pressure. Black stars represent data for a polymer membrane with "exceptional performance" recently reported in *Science* [5]. The original figure is obtained from [4], with permission from Elsevier.

temperature of 67 K. This membrane performance is well above the 2008 upper bound in the Robeson selectivity–permeability plot for polymeric membranes at room temperature [4], see Fig. 6. The separation performance at the other investigated feed pressures (400 mbar, 660 mbar and 1000 mbar) also lies well above the upper bound. The performance of our membrane (in terms of selectivity and permeability) is comparable to that recently reported by Carta et al. [5] for novel polymeric membranes. However, it is worth pointing out that the measured O_2 permeance for our thin MFI membrane is more than 100 times larger than that for the polymeric membranes (lower than 5.5×10^{-9} mol m^{-2} s^{-1} Pa^{-1}) with a thickness ranging from 95 to 181 μm [5].

Fig. 7a shows the maximum O_2/N_2 separation factors observed at the optimum separation temperature at each feed pressure. The maximum O_2/N_2 separation factors increased significantly as the feed pressure was decreased from 1000 mbar to 100 mbar. In addition, the optimum separation temperatures decreased as the feed pressure was increased. For instance, the maximum separation factor was only 3.7 at the optimum temperature of 89 K when the feed pressure was 1000 mbar, whereas the maximum separation factor observed at 67 K and at a feed pressure of 100 mbar was 5.0. As discussed above, the separation is most probably governed by O_2/N_2 adsorption selectivity, and this selectivity is higher at low temperatures.

Fig. 7b shows permeances of O_2 and N_2 measured in the gas mixture separation experiments at the optimum separation temperatures as a function of pressure. The figure also shows O_2/N_2 membrane selectivities at the optimum separation temperatures. The permeance of O_2 was higher than that of N_2 in the entire feed pressure range. Accordingly, the O_2/N_2 membrane selectivities, defined as the ratio of O_2 permeance over N_2 permeance, were above unity at all feed pressures, which shows that the membrane was oxygen selective. Both O_2 and N_2 permeances observed in the present work showed no strict correlation with the feed pressures. However, the membrane selectivity increased as the feed pressure and temperature was decreased. This is consistent with the results from the previous

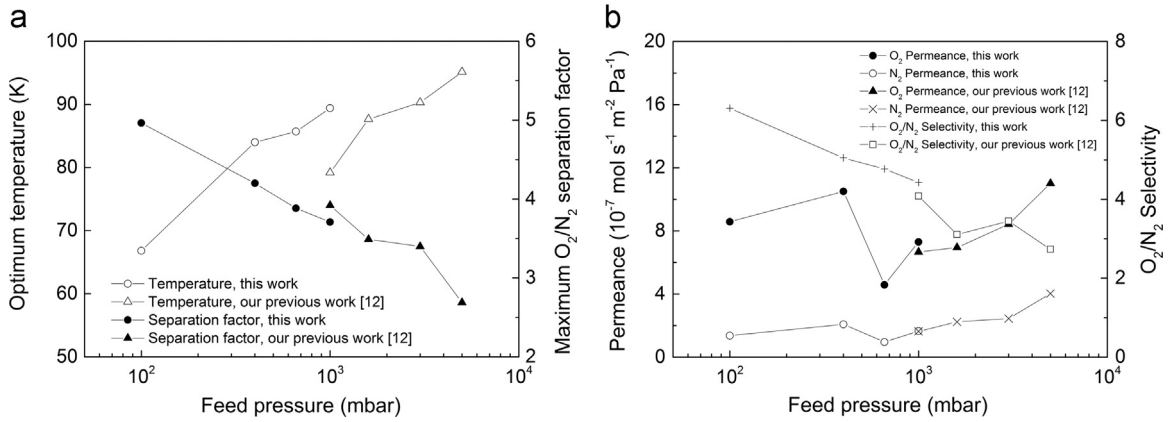

Fig. 7. (a) Optimum separation temperatures and maximum O_2/N_2 separation factors as a function of feed pressure. (b) Permeances of O_2 and N_2 measured in the gas mixture separation experiments at optimum separation temperatures as a function of feed pressure.

work [12]. An entirely opposite situation was observed in the single gas permeation experiments (see Fig. 5) i.e., the permeance of O_2 was lower than that of N_2 at all temperatures. Furthermore, the N_2 permeance measured in the gas mixture separation experiments was much lower, by ca. a factor of 7, than that measured in the single gas permeation experiments. In contrast, the O_2 permeances were comparable. The observations in the present work are consistent with those reported in our previous work [12] using feed pressures ranging from 1 bar to 5 bar. The slightly higher selectivity (at a higher optimum temperature) for a feed pressure of 1 bar in present work compared to the previous work might emanate from the experimental differences. Helium was used as a sweep gas in the previous work, while no sweep gas was used in the present work. Counter diffusion of helium may certainly influence the separation performance to some extent.

5. Conclusions

For the first time, ultra-thin MFI membranes were evaluated at cryogenic temperature for air separation at low feed pressure down to 100 mbar. The membranes were found to be oxygen selective at all the conditions studied. The observed O_2/N_2 selectivity and oxygen permeance were well above the upper bound in the 2008 Robeson selectivity–permeability plot. The permeance was nearly 100 times higher than that recently reported for promising polymeric membranes. The selectivity to O_2 should primarily emanate from O_2/N_2 adsorption selectivity. In addition, with decreasing feed pressure and temperature, the O_2/N_2 membrane selectivity was found to increase, which can most likely be attributed to greater O_2/N_2 adsorption selectivity at lower temperatures. The present work has therefore indicated the optimum conditions for air separation using MFI membranes, namely low feed pressures and low temperatures.

Acknowledgments

The Swedish Research Council (Grant no. RMA08-0018), the Swedish Foundation for Strategic Research (Grant no. 2010-5317) and the Swedish Energy Agency (Grant no. 2013-006587) are gratefully acknowledged for financially supporting this work. Furthermore, the authors are grateful to Göran Wallin for technical assistance.

References

[1] P. Bernardo, E. Drioli, G. Golemme, Membrane gas separation: a review/state of the art, Ind. Eng. Chem. Res. 48 (2009) 4638.
[2] R. Baker, Membrane Technology and Applications, John Wiley and Sons, England, 2004.
[3] L.M. Robeson, Correlation of separation factor versus permeability for polymeric membranes, J. Membr. Sci. 62 (1991) 165.
[4] L.M. Robeson., The upper bound revisited, J. Membr. Sci. 320 (2008) 390.
[5] M. Carta, R. Malpass-Evans, M. Croad, Y. Rogan, J.C. Jansen, P. Bernardo, et al., An efficient polymer molecular sieve for membrane gas separations, Science 339 (2013) 303.
[6] M. Hong, S. Li, J.L. Falconer, R.D. Noble, Hydrogen purification using a SAPO-34 membrane, J. Membr. Sci. 307 (2008) 277.
[7] E. Piera, C.A.M. Brenninkmeijer, J. Santamaría, J. Coronas, Separation of traces of CO from air using MFI-type zeolite membranes, J. Membr. Sci. 201 (2002) 229.
[8] J. van den Bergh, W. Zhu, J. Gascon, J.A. Moulijn, F. Kapteijn, Separation and permeation characteristics of a DD3R zeolite membrane, J. Membr. Sci. 316 (2008) 35.
[9] J. Hedlund, J. Sterte, M. Anthonis, A. Bons, B. Carstensen, N. Corcoran, et al., High-flux MFI membranes, Microporous Mesoporous Mater. 52 (2002) 179.
[10] L. Sandström, E. Sjöberg, J. Hedlund, Very high flux MFI membrane for CO_2 separation, J. Membr. Sci. 380 (2011) 232.
[11] M. Zhou, D. Korelskiy, P. Ye, M. Grahn, J. Hedlund., A uniformly oriented MFI membrane for improved CO_2 separation, Angew. Chem. Int. Ed. 53 (2014) 3492.
[12] P. Ye, E. Sjöberg, J. Hedlund, Air separation at cryogenic temperature using MFI membranes, Microporous Mesoporous Mater. 192 (2014) 14.
[13] J. Hedlund, F. Jareman, A. Bons, M. Anthonis., A masking technique for high quality MFI membranes, J. Membr. Sci. 222 (2003) 163.
[14] J. Hedlund, D. Korelskiy, L. Sandström, J. Lindmark, Permporometry analysis of zeolite membranes, J. Membr. Sci. 345 (2009) 276.
[15] D. Korelskiy, M. Grahn, J. Mouzon, J. Hedlund, Characterization of flow-through micropores in MFI membranes by permporometry, J. Membr. Sci. 417–418 (2012) 183.
[16] D. Korelskiy, P. Ye, H. Zhou, J. Mouzon, J. Hedlund., An experimental study of micropore defects in MFI membranes, Microporous Mesoporous Mater. 186 (2014) 194.
[17] G. Sethia, R.S. Pillai, G.P. Dangi, R.S. Somani, H.C. Bajaj, R.V. Jasra, Sorption of methane, nitrogen, oxygen, and argon in ZSM-5 with different SiO_2/Al_2O_3 ratios: grand canonical monte carlo simulation and volumetric measurements, Ind. Eng. Chem. Res. 49 (2010) 2353.
[18] F.R. Siperstein, Determination of azeotropic behavior in adsorbed mixtures, Adsorption 11 (2005) 55.
[19] T. Nitta, T. Shigetomi, M. Kuro-oka, T. Katayama, Adsorption isotherm of multi-site occupancy model for homogeneous surface, J. Chem. Eng. Jpn. 17 (1984) 39.
[20] D.D. Do, Adsorption Analysis: Equilibria and Kinetics, World Scientific, Singapore, 1998.
[21] R. Krishna, J.M. van Baten., Maxwell–Stefan modeling of slowing-down effects in mixed gas permeation across porous membranes, J. Membr. Sci. 383 (2011) 289.